Hindawi
Advances in Materials Science and Engineering
Volume 2022, Article ID 8274733, 15 pages
https://doi.org/10.1155/2022/8274733

Research Article

Experimental Research on Mix Ratio of Construction Waste Cemented Filling Material Based on Response Surface Methodology

Weixin Chen, Guohua Zhang, Qin Tao, Liangliang Yu, Tao Li, and Xianhua Guan

School of Mining Engineering, Heilongjiang University of Science and Technology, D2468 Puyuan Road, Harbin 150022, China

Correspondence should be addressed to Weixin Chen; cwxkygcxy@163.com

Received 25 April 2022; Accepted 8 June 2022; Published 14 July 2022

Academic Editor: Bowen Guan

Copyright © 2022 Weixin Chen et al. This is an open access article distributed under the Creative Commons Attribution License, which permits unrestricted use, distribution, and reproduction in any medium, provided the original work is properly cited.

In order to solve the problem of insufficient supply of aggregate for cemented filling material, the experimental research on the mix ratio of cemented filling material using construction waste as recycled coarse aggregate was carried out. A ternary quadratic regression model was created using the Box-Behnken design (BBD) based on the response surface methodology (RSM), using slump, bleeding ratio, and 28 d uniaxial compressive strength of the filling material as response variables, and the model's accuracy and reliability were confirmed. The findings of the regression model reveal that the response value is influenced by a single component as well as the interaction between the two factors. Finally, based on filling material cost optimization model, an optimal mix ratio is given, in which the wet fly ash/aggregate ratio, Talbol gradation index of recycled aggregate, and dosage of water reducing agent to cement are 0.507, 0.5, and 0.678%, respectively. The filling material which adopted the optimal mix ratio exhibited a good performance with slump of 215 mm and bleeding ratio of 4.00%, uniaxial compressive strength increased significantly within 3 d, and 28 d uniaxial compressive strength was 4.08 MPa, which meet the requirements of field construction.

1. Introduction

Coal, as an important natural resource, plays a significant role in industrial production and daily life. However, coal mining activities give rise to a series of environmental problems, such as ecological environment destruction, stratum instability, surface subsidence, and groundwater loss. In order to address these issues, abundant studies and practices have been conducted, yielding many effective solutions. In recent years, the development of human society has been calling for the environmental, safe, and harmless technologies and methods [1, 2]. It has been proved in practice that filling mining is an effective way to achieve this goal in coal mining [3–5].

Currently, the common filling materials for coal mining include waste gangue, paste, and high water material. Beside the expensive prices, the insufficient supply of these raw materials for filling is also a key factor restricting the large-scale application of filling mining [6–10]. In the process of urban construction, huge amount of construction waste has been produced. Specifically, the construction waste accounts for 30~40% of the total amount of urban waste in China, which is relatively large [11, 12]. Since 2012, the amount of new construction waste in China reached over 1 billion tons per year, though its reutilization rate was no more than 10% [13, 14]. Undoubtedly, this construction waste, in such a large amount, will cause harmful impacts on the ecological environment if without proper handling. In view of this, the reutilization of construction waste is an effective way to solve the problems. Therefore, construction waste is made into recycled aggregates and mixed with cemented materials to form new cemented filling material, so as to meet the needs of the industry, which can effectively save the cost and solve the raw material shortage for mine filling, as well as realizing resource conservation and ecological environment protection.

In recent years, the research about filling material containing construction waste recycled aggregate has been a hot topic. Based on the orthogonal experiment, Liu et al. [15] took construction waste, quick lime, gypsum, and the coarse fly ash as cemented material to analyze the influence of various factors on property indexes of filling mortar and derived the optimal ratio of construction waste to filling material. The result exhibited that mortar mass concentration and cement-aggregate ratio are the main influential factors for the delamination degree and compressive strength of the filling body. Zhang et al. [16] studied three kinds of construction waste; ordinary silicate cement and fly ash formulated into paste materials basically meet the requirements of filling, among which the frame structure construction waste paste material has better performance. Jiang et al. [17] determined the optimal mixture proportion of mortar filling material composed of construction waste, natural sand, ordinary Portland cement, and fly ash through the orthogonal test. Qiu et al. [18] studied the preparation of cementitious filling material with construction waste, silicate cement, water ash, and additives and analyzed the strength and microstructural changes of the filling material with different particle sizes of construction waste. Li et al. [19] used quicklime, gypsum, compound early strength agent, coarse fly ash, and construction waste as the raw materials for the filling material and used orthogonal tests to determine the optimum ratio of the filling material and to analyze the mechanical properties of the construction waste-coarse fly ash-based binder filling body. Liu et al. [20] analyzed the aggregate particle size distribution, compressive strength, and fine structure of cementitious paste fillings prepared from construction waste and ordinary silicate cement. Yang et al. [21] established the regression models by using the RSM optimization method to explore the effects of the concentration and suspension agent on the properties of coal gangue and silicate cement based cementitious filling material and finally obtained an optimal mix ratio. Tang et al. [22] used the RSM-DDC (the central-composite design based on the response surface methodology) method to study the mechanical properties of the filling material ratio with coal gangue as aggregate and Portland cement as cementitious materials, assessed the influence of each component on the properties, and got the optimal ratio with the coal-based solid waste consumption of 91.5%.

Although there has been much research on construction waste filling material, few papers have focused on experimental investigation of construction waste filling material utilizing the RSM-BBD (the Box-Behnken design based on the response surface methodology) approach. In addition, in previous studies, the main cementitious materials for filling material were silicate cement, lime, gypsum, and so forth. This paper makes an attempt to prepare filling material from tiny quantities of sulphate aluminium cement and silicate cement as cementitious materials with construction waste, fly ash, water reducing agents, and water and to use the response method implemented by the Box-Behnken module of the Design-Expert software. This work can improve the early strength of filling material as much as possible under the premise of meeting the performance requirements of filling material, considering the cost factor, and finally obtaining the final mix ratio of construction waste cemented filling material. The research can reference the field application of construction waste cemented filling material.

2. Materials and Methods

2.1. Materials

2.1.1. Construction Waste. The construction waste (Figure 1), mainly composed of fragment concrete, mortar, bricks, and tiles, was used as recycled aggregate, whose density is 2.62 g/cm^3. Clear construction waste was collected by two stages of crush at Harbin Jinlu Renewable Resources Co., Ltd, and it was sieved into five particle size ranges: 0~2.5 mm, 2.5~5 mm, 5~10 mm, 10~16 mm, and 16~20 mm. The Talbol continuous gradation equation was used to calculate the mass ratio of the construction waste in each particle size range of samples, with the following expression:

$$P = 100 \times \left(\frac{d}{D}\right)^n, \quad (1)$$

where n is Talbol grading index; d is the particle size of crushed construction waste, mm; D is the maximum particle size of crushed construction waste, mm; P is the mass percentage of crushed construction waste with the particle size less than D, %.

Talbol gradation index (n) of the broken construction waste is 0.65 (Figure 2). When Talbol gradation index (n) of the aggregate ranges between 0.3 and 0.5, the materials mixed will be more uniform, with high bulk density and strength [23]. So the aggregates with Talbol gradation indexes (n) of 0.3, 0.4, and 0.5 were taken as experimental objects. Aggregates with various Talbol gradation indexes are listed in Table 1.

2.1.2. Wet Fly Ash. The abandoned wet fly ash of Qitaihe Gangue Thermal Power Plant has moisture content of 42%. The chemical composition of fly ash [24] is shown in Table 2. The SEM photos show that the fly ash has major irregular shape, massive block granules, and rare spherical glass beads (Figure 3). The Talbol gradation index n of fly ash is 0.47 (less than 0.5, Figure 4), indicating good gradation and high bulk density.

2.1.3. Cement. The cement used in the experiments was 42.5$^{\#}$ sulphate aluminate cement and 42.5$^{\#}$ Portland cement mixed at a mass ratio of 3 : 10, with density of 3.1 g/cm^3. The fineness of mixed cement measured by specific surface area is 3100–3300 cm^2/g. The initial setting time of mixed cement is more than 30 minutes, and the final setting time is less than 5 hours.

2.1.4. Water Reducing Agent. Polycarboxylic acid water reducing agent with density of 2.1 cm^3/g can reduce 35% of water, and gas increase is less than 6%. The 28-day strength of cement can be increased by more than 30%.

Figure 1: Appearance of construction waste.

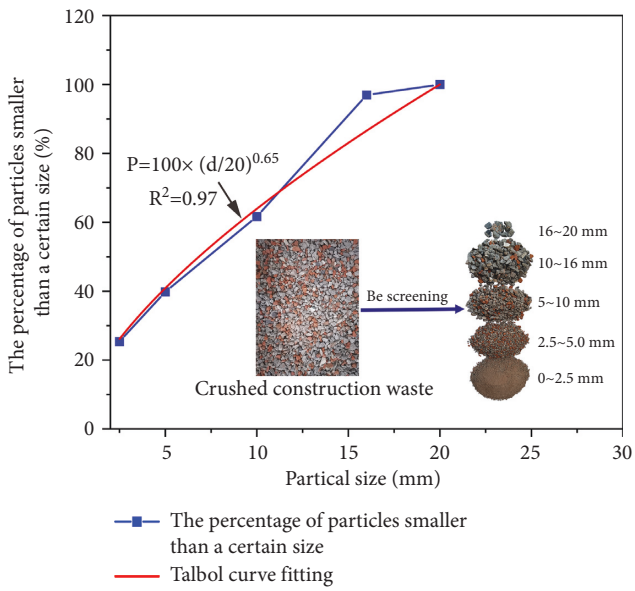

Figure 2: Particle size grading curve of crushed construction waste.

2.2. Experimental Design Method. In this paper, Box-Behnken design (BBD) based on the response surface methodology (RSM) was conducted by using Design-Expert 10.0.3 software [21]. In the Box-Behnken design, wet fly ash/construction waste ratio, Talbol gradation index of construction waste, and usage of water reducing agent were taken as independent variables. Table 3 shows different levels in the form of actual and coded values. The slump, bleeding ratio, and uniaxial compressive strength of filling material were taken as dependent variables. The multivariate nonlinear regression fitting of these data was performed by the Design-Expert 10.0.3 software. The established regression model is

$$Y_n = a + \sum_{j=1}^{m} b_j x_j + \sum_{j=1}^{m} b_{kj} x_j^2 + \sum_{k<j} b_{jj} x_k x_j + e(X_1, X_2, \ldots X_3), \quad (2)$$

where Y_n represents the dependent variable; a is constant; b_j, b_{kj}, and b_{jj} are the linear, quadratic, and interaction coefficients, respectively; x_j and x_k are the coded values of independent parameters; e denotes the error caused by test and regression.

2.3. Mix Ratios. In this paper, on the basis of the filling mining practice of Longhu mine in Qitaihe, the approximate proportion range of the experimental level of raw materials is determined. When the solid mass concentration is 75% and the cement content is 8% of the total weight, the 28 d uniaxial compressive strength of the material is greater than 3 MPa, which can meet the strength requirements of Longhu mine for filling material. The horizontal selection of the mass ratio of wet fly ash to construction waste x_1, Talbol grading index x_2 of construction waste, and the mass percentage of water reducing agent in cement x_3 are shown in Table 3. During the experiment, 17 mix ratios were tested, as listed in Table 4.

2.4. Testing and Evaluation Methodology

2.4.1. Slump Test. Filling slurry was added to a moist slump cone by three times, and a third amount of slurry was added each time. Each layer was rammed 25 times with a ramming bar. When adding the top layer, the filling slurry should be higher than the top of the slump cone, and the excess filling slurry was scraped off with a spatula. Then the slump cone was lifted vertically and smoothly. The level difference between the height of slump cone and the highest point of the filling slurry tested is the slump value of filling slurry (Figure 5).

2.4.2. Bleeding Ratio Test. Firstly, filling slurry was added to a 5 L covered barrel (inner diameter of 185 mm and height of 200 mm) and vibrated on the vibration table for 20 s, of which surface was wiped gently with a spatula and covered to prevent moisture evaporation. The surface level of the slurry was 20 mm lower than the edge of the barrel. After the filling slurry was smoothed, bleeding water was pumped out by a straw every 10 mins once for the first 60 mins and every 20 mins once later until there was no bleeding water for three times (Figure 6). The water pumped out was injected in a measuring cylinder with a plug, and the total amount of water was accumulated. The bleeding ratio is calculated by the following formula:

$$B = \frac{W_W}{(w/m) \times (m1 - m0)} \times 100\%, \quad (3)$$

where B is the bleeding ratio (%); W_W is the accumulated amount of water (g); m is the total weight of filling slurry (g); w is the total weight of water (g); m_1 is the initial total weight of barrel and loaded filling slurry (g); m_0 is the weight of barrel (g).

2.4.3. Uniaxial Compressive Strength Test. Three $10 \times 10 \times 10\ cm^3$ cube specimens of filling material were made as a group. The filling slurry was loaded into the mold and vibrated for 20 s. Then excess filling slurry at the top of mold was scraped off, and the surface of specimen was smoothed. These specimens were put into the standard curing box for 28 d (Figure 7). After that, these specimens were taken out and the mold was removed for uniaxial

Table 1: Particle size distribution of construction waste for different Talbol gradation indexes (wt. %).

n	Particle size range (mm)				
	<2.5	2.5~5	5~10	10~16	16 ~20
$n = 0.3$	53.59	12.39	15.25	12.30	6.48
$n = 0.4$	43.53	13.91	18.35	15.68	8.54
$n = 0.5$	35.36	14.64	20.71	18.73	10.56

Table 2: Chemical composition and physical properties of fly ash.

	SiO_2	Al_2O_3	Fe_2O_3	CaO	MgO	K_2O	Na_2O	SO_3	Loss	Total	Fineness (m^2/kg)	Density (kg/m^3)
Fly ash	37.2	24.5	8.4	8.3	1.6	1.2	1.6	12.2	2.7	97.7	119.0	2.2

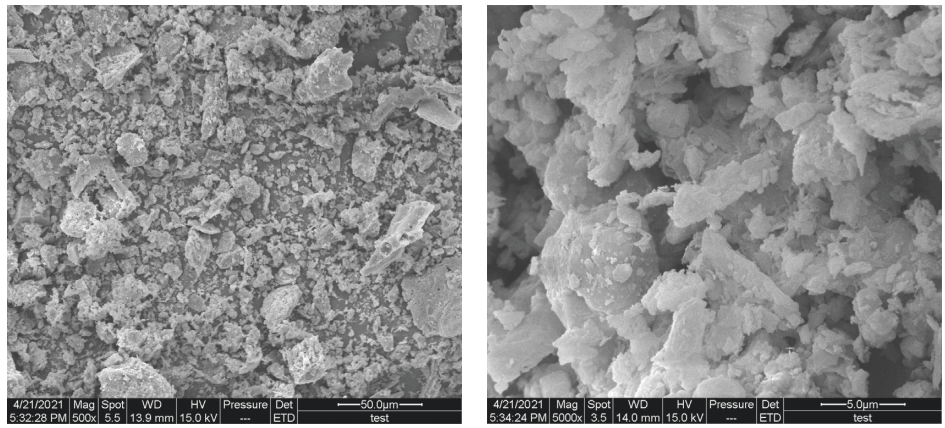

(a) (b)

Figure 3: SEM photos of fly ash. (a) 500 times of SEM photo. (b) 5000 times of SEM photo.

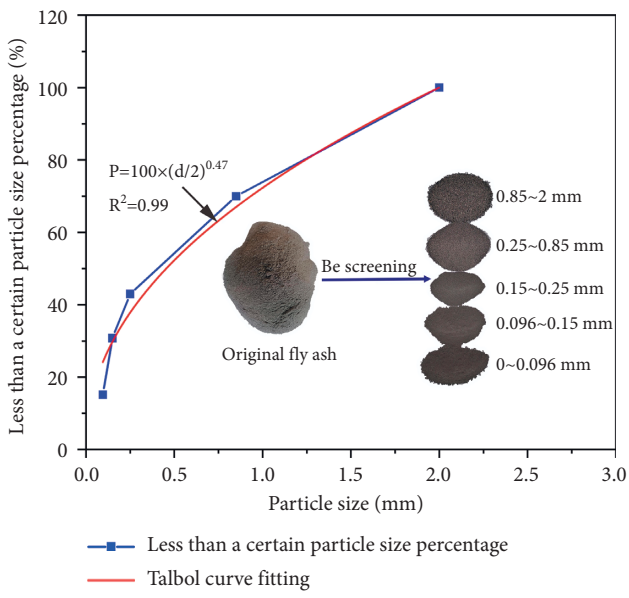

Figure 4: Particle size gradation curve of fly ash.

compressive strength test. YAW-300 microcomputer controlled automatic concrete pressure testing machine was used for test. In test process, the bearing surface of the specimen should be vertical to the top surface of the specimen, and the center of specimen was aligned with the center of the pressing plate. The press was boosted continuously at the loading speed of 0.002 mm/s until yield failure occurred in the specimen, and the maximum was recorded as the failure load (Figure 7(b)). The compressive strength (σ_c) of specimen was calculated according to the following formula:

$$\sigma_c = \frac{F}{A}, \tag{4}$$

where F is failure load (N) and A is compression area (mm^2).

3. Results and Discussion

3.1. Model Fitting and Analysis. The results of tests are listed in Table 5.

In this study, the acceptance probability of coefficients (P) was less than 0.05. To ensure the accuracy of the model, the insignificant terms with P value of the independent variable coefficient greater than 0.05 were eliminated. The response surface functions of slump, bleeding ratio, and 28 d uniaxial compressive strength were obtained. The final equations in terms of the coded factors are listed as follows.

Table 3: Actual and coded values of the experimental factors.

Wet fly ash/construction waste ratio	Talbol gradation index of construction waste	The percentage of water reducing agent in cement (%)	Coded value
x_1	x_2	x_3	
0.45	0.3	0.6	1
0.50	0.4	0.7	0
0.55	0.5	0.8	−1

Table 4: Mix ratios of filling material for orthogonal test.

Samples	Wet fly ash (wt. %)	Construction waste (wt. %)	Talbol gradation index	Sulphate aluminate cement (wt. %)	Portland cement (wt. %)	Water reducing agent (wt. %)	Water (wt. %)
1#	20.78	46.17	0.5	2.4	5.6	0.56	25.0
2#	22.31	44.63	0.4	2.4	5.6	0.56	25.0
3#	23.76	43.19	0.4	2.4	5.6	0.48	25.0
4#	22.31	44.63	0.4	2.4	5.6	0.56	25.0
5#	22.32	44.63	0.5	2.4	5.6	0.48	25.0
6#	22.31	44.62	0.5	2.4	5.6	0.64	25.0
7#	23.75	43.19	0.3	2.4	5.6	0.56	25.0
8#	20.78	46.17	0.4	2.4	5.6	0.48	25.0
9#	22.32	44.63	0.3	2.4	5.6	0.48	25.0
10#	23.75	43.18	0.4	2.4	5.6	0.64	25.0
11#	22.31	44.63	0.4	2.4	5.6	0.56	25.0
12#	22.31	44.63	0.4	2.4	5.6	0.56	25.0
13#	20.77	46.16	0.4	2.4	5.6	0.64	25.0
14#	23.75	43.19	0.5	2.4	5.6	0.56	25.0
15#	20.78	46.17	0.3	2.4	5.6	0.56	25.0
16#	22.31	44.63	0.4	2.4	5.6	0.56	25.0
17#	22.31	44.62	0.3	2.4	5.6	0.64	25.0

Slump:

$$Y_1 = 211.89 - 3.25x_1 + 3.63x_2 + 5.63x_3 + 1.75x_1x_2 - 20.01x_1^2 - 3.76x_2^2. \quad (5)$$

Bleeding ratio:

$$Y_2 = 4.30 - 0.81x_1 + 0.27x_2 + 0.30x_3 - 0.094x_1x_2 - 0.48x_1^2 - 0.38x_2^2. \quad (6)$$

28 d compressive strength:

$$Y_3 = 3.66 + 0.063x_1 + 0.25x_2 - 0.088x_3 + 0.1x_1x_2 - 0.17x_1x_3 - 0.12x_1^2 + 0.16x_2^2 - 0.17x_3^2. \quad (7)$$

To investigate the interaction influence between factors based on the response surface regression model and the response values, variance analysis was conducted on the error sources of the regression equation, as shown in Table 6. The significance of the model is determined by F value and P value: the higher F value and lower P value indicate a significant influence. The F values of the regression model are 180.35, 197.19, and 70.72, respectively, with the P values far less than 0.0001, indicating a significant influence of the regression model. The orders of significance of the single factors on response values (Y_1, Y_2, and Y_3) are $x_3 > x_2 > x_1$, $x_1 > x_3 > x_2$, and $x_2 > x_3 > x_1$, respectively. The order of significance of interaction effect on 28 d compressive strength is $x_1x_3 > x_1x_2$. The determination coefficient determined by the model can explain the degree of difference between the response surface and the real value. Therefore, the determination coefficient determined by the model is used to evaluate the accuracy and reliability of the regression model [25], as shown in Table 7. If the determination coefficient (R^2) and coefficient of variation (CV) are close to 1 and 0, respectively, the model is of high reliability. For the three models, the determination coefficient (R^2), adjusted determination coefficient (R^2_{Adj}), and predictive determination coefficient (R^2_{pred}) are greater than 0.93, and all the coefficients of variation (CV) are less than 5%, indicating that the models are reliable and accurate (Table 7).

In order to directly express the accuracy of the model, a three-dimensional error coordinate system was constructed, in which the relative differences between the measured value Y and the calculated value Y' of x_1, x_2, and x_3 are plotted (Figure 8). As shown in Figure 8, the relative errors of slump, bleeding ratio, and 28 d compressive strength, are less than 1.5%, 4%, and 1.5%, respectively [26], which means the calculated values of the models are close to the actual values, indicating a high accuracy of the models.

3.2. Properties Analysis of Filling Material. In this study, the established model was used to explain the influence of various independent variables and their binary interactions

(a) (b)

Figure 5: Photos of slumps test. (a) Measuring device. (b) Slump measurement.

(a) (b)

Figure 6: Photos of bleeding ratio test. (a) Measuring device. (b) Bleeding ratio measurement.

on the response values, namely, properties of filling material. The details are discussed as follows.

3.2.1. Analysis of Single Factor Influence on Response Value

(1) Analysis of Factors Influencing Slump. In response surface methodology regression model, according to the results of ANOVA, slump is significantly influenced by single factors. The influence of each factor on slump is shown in Figure 9(a). When analyzing the influence of a single factor on slump, the other two factors are fixed at the code level of 0 (i.e., wet fly ash/aggregate ratio of 0.5 or Talbol gradation index of 0.4 or water reducing agent of 0.7, the same as follows). With the increase of wet fly ash content, slump value increases at the beginning and then decreases. In relevant literature [27], there is a similar rule, but the threshold value is 30%, which may be increased due to the coarse particle size of wet fly ash. With the increase of Talbol gradation index of construction waste (N), the slump first obviously increases and then slightly decreases or remains as is. Water reducing agent can increase the fluidity of filling material. Therefore, with the increase of water reducing agent proportion, slump would increase continuously, but the increase rate of slump shows a decreasing trend. It proves that the water reducing agent accounts for a lasting impact on the fluidity of filling material within the permissible amount.

(2) Analysis of Factors Influencing Bleeding Ratio. The influence of each factor on bleeding ratio is shown in Figure 9(b). With the increase of wet fly ash/aggregate ratio, the bleeding ratio remains as is at first and then decreases. When the code value of wet fly ash/aggregate ratio exceeds −0.50, the decreasing range of bleeding becomes more obvious. Wet fly ash can make up for the shortage of fine aggregate in cement and construction waste, so as to reduce the water usage and block the bleeding channel, thus decreasing the bleeding ratio and improving the antiseepage ability of filling material [27, 28]. When the proportion of

(a) (b)

Figure 7: Photos of stress resistance test. (a) The test specimens. (b) Compressive strength measurement.

Table 5: The results of tests.

Samples	Slump (mm)	Bleeding ratio (%)	28 d compressive strength (MPa)
1#	193	4.63	3.8
2#	213	4.38	3.7
3#	183	2.63	3.7
4#	212	4.25	3.7
5#	206	3.75	4
6#	217	4.50	3.8
7#	181	2.50	3.4
8#	190	4.38	3.2
9#	196	3.38	3.5
10#	192	3.25	3.2
11#	212	4.38	3.7
12#	213	4.38	3.6
13#	200	4.88	3.4
14#	191	2.88	4.1
15#	190	3.88	3.5
16#	212	4.25	3.6
17#	211	3.88	3.3

water reducing agent increases, the bleeding ratio increase continuously, showing a linear correlation between them. The water reducing agent changes the ratio of bound water, adsorption water, and free water and improves the free water content. Therefore, the excess free water bleeds at first, thus increasing the rate of bleeding. There are both positive and negative effects of gradation on bleeding ratio. When the code value of Talbol gradation index is 0.425, the bleeding ratio reaches the maximum; when the index is less than 0.025, the bleeding ratio increases with the increase of the index; when the index is above 0.025, the bleeding ratio decreases with the increase of the index, but the increment is more obvious than the decrement.

(3) 28 d Compressive Strength. The influence of various factors on 28 d compressive strength is shown in Figure 9(c). With the increase of wet fly ash/aggregate ratio, the 28 d compressive strength of filling material increases first and then basically remains constant and finally decreases. When the code of wet fly ash/aggregate ratio is between 0.21 and 0.23, the 28 d compressive strength remains basically stable. Before that, the compressive strength increases with the increase of the ratio. After the maximum value, the compressive strength declines as the ratio increases. The effect of gradation on compressive strength exhibits a fixed value when the Talbol gradation index code is below −0.178. Subsequently, with the increase of Talbol grading index, the compressive strength increases. It indicates that the coarse aggregate content is conducive to the increase of compressive strength. When the water reducing agent usage is less than 0.071, the compressive strength increases with the increase of water reducing agent content. After that, the compressive strength decreases with the increase of the proportion of water reducing agent. It proves that the rational use of polycarboxylic acid water reducing agent will increase the compressive strength of filling material, but too much water reducing agent will decrease the compressive strength of filling material.

3.2.2. Analysis of Interaction Influence on Response Value. According to the test results and variance analyses, it can be seen that the response values are affected not only by a single

Table 6: Results of ANOVA.

Source	Sum of squares	d_f	Mean square	F value	P value prob > F	
Slump						
Model	2246.77	6	374.46	180.35	<0.0001	Significant
x_1	84.50	1	84.50	40.70	<0.0001	
x_2	105.13	1	105.13	50.63	<0.0001	
x_3	253.13	1	253.13	121.91	<0.0001	
x_1x_2	12.25	1	12.25	5.90	0.0355	
x_1^2	1691.11	1	1691.11	814.48	<0.0001	
x_2^2	59.79	1	59.79	28.80	0.0003	
Bleeding rate						
Model	5.29	6	0.8822	197.19	<0.0001	Significant
x_1	3.38	1	3.38	755.53	<0.0001	
x_2	0.3613	1	0.3613	80.75	<0.0001	
x_3	0.4512	1	0.4512	100.87	<0.0001	
x_1x_2	0.0225	1	0.0225	5.03	0.0488	
x_1^2	0.6190	1	0.6190	138.37	<0.0001	
x_2^2	0.4003	1	0.4003	89.47	<0.0001	
28 d compressive strength						
Model	1.03	8	0.1282	70.72	<0.0001	Significant
x_1	0.0313	1	0.0313	17.24	0.0032	
x_2	0.5000	1	0.5000	275.86	<0.0001	
x_3	0.0613	1	0.0613	33.79	0.0004	
x_1x_2	0.0400	1	0.0400	22.07	0.0015	
x_1x_3	0.1225	1	0.1225	67.59	<0.0001	
x_1^2	0.0581	1	0.0581	32.07	0.0005	
x_2^2	0.1044	1	0.1044	57.63	<0.0001	
x_3^2	0.1181	1	0.1181	65.18	<0.0001	

Table 7: Model correlation evaluation.

Evaluation index	Y_1	Y_2	Y_3
Determination coefficient (R^2)	0.995	0.992	0.986
Adjusted determination coefficient (R^2_{Adj})	0.990	0.987	0.972
Predictive determination coefficient (R^2_{pred})	0.930	0.970	0.951
Coefficient of variation (CV)	0.610%	2.150%	1.18%

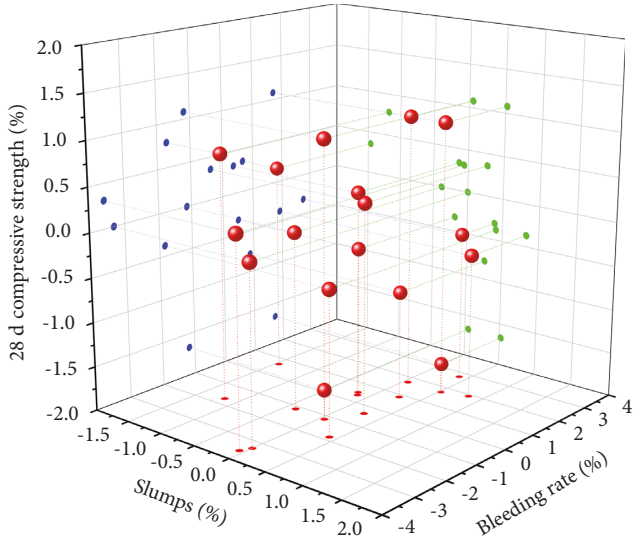

Figure 8: Three-dimensional error coordinate system of the regression model.

factor but also by the interaction between factors, which is discussed in detail as follows.

In Figure 10, when the percentage of water reducing agent is 0.7%, the slump shows a trend of gradual increase with the increase of wet fly ash/aggregate ratio before 0.49 at the aggregate gradation of 0.3. When wet fly ash/aggregate ratio is 0.49, it reaches the maximum and then presents a declining trend, with the rate of decline slightly higher than the increase rate. When the wet fly ash/aggregate ratio is fixed, the slump obviously increases at first and then decreases with the increase of gradation. The effect of gradation on slump is lower than that of the wet fly ash/aggregate ratio, which is consistent with the result of variance analysis. In addition, the contour map is oval, indicating a strong interaction between mass and cement dosage [29]. In a word, when the gradation and wet fly ash/aggregate ratio vary, slump values show a parabolic regularity on the coordinate axes. Suitable aggregate gradation and wet fly ash/aggregate ratio can adjust the slump of filling material to reach a reasonable engineering range.

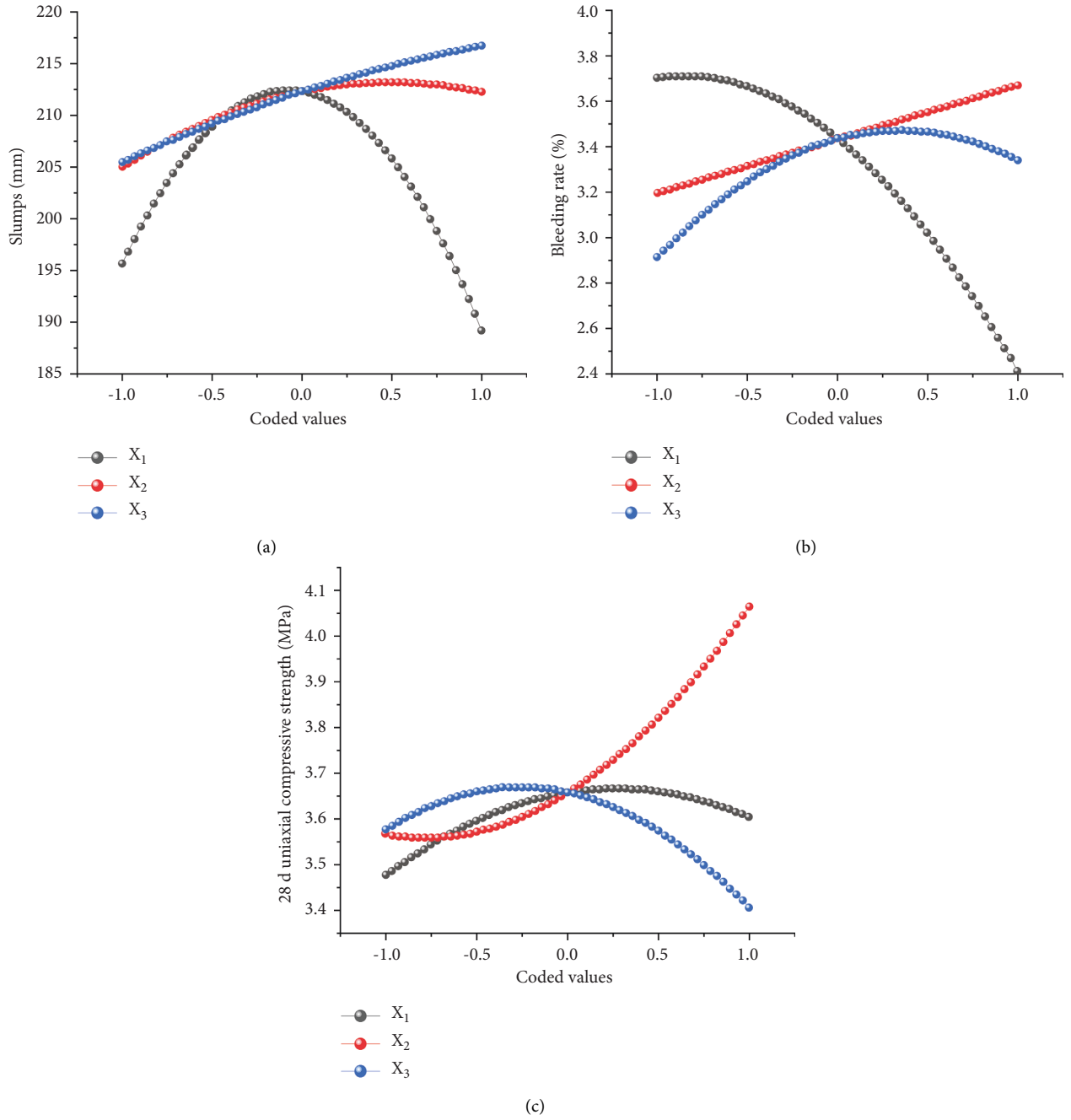

Figure 9: Influence curve of single factors on each response value. (a) Slump. (b) Bleeding ratio. (c) 28 d compressive strength.

In Figure 11, when the percentage of water reducing agent is 0.7%, the bleeding ratio of filling material shows a slight increase with the increase of wet fly ash/aggregate ratio and reaches the maximum of 3.9% at the wet fly ash/aggregate ratio of 0.46. After that, the bleeding ratio declines to 2.45% at last, indicating a significant influence of wet fly ash/aggregate ratio on the bleeding ratio. When Talbol gradation index of construction waste is 0.5, with the increase of wet fly ash/aggregate ratio, the bleeding ratio decreases sharply, from 4.63% to 2.79%, reaching a variation of 40%. At a low wet fly ash/aggregate ratio, with the increase of the index, the bleeding ratio increases from 3.88% to 4.72% and then remains as is. When the wet fly ash/aggregate ratio is 0.55, with the increase of gradation, the bleeding rate increases from 2.45% to 3.02% and then decreases to 2.79%, indicating that the influence of gradation on bleeding rate can be reduced with the increase of wet fly ash/aggregate ratio. In addition, according to the contour diagram (Figure 11(a)), when the Talbol grading index of construction waste and wet fly ash/aggregate ratio are in the ranges of 0.3 to 0.39 and 0.53 to 0.55, respectively, the bleeding ratio is low.

In Figure 12, when the percentage of water reducing agent is 0.7% with the gradation of construction waste fixed, 28 d compressive strength increases first and then decreases

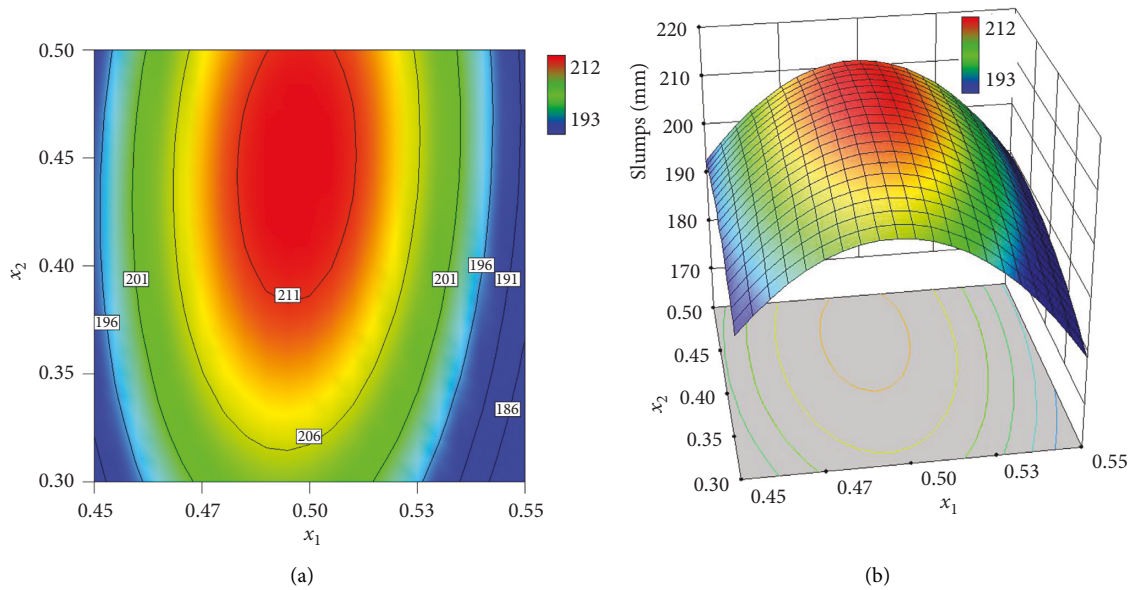

Figure 10: Interaction influence of x_1 and x_2 on slump. (a) Two-dimensional diagram. (b) Three-dimensional diagram.

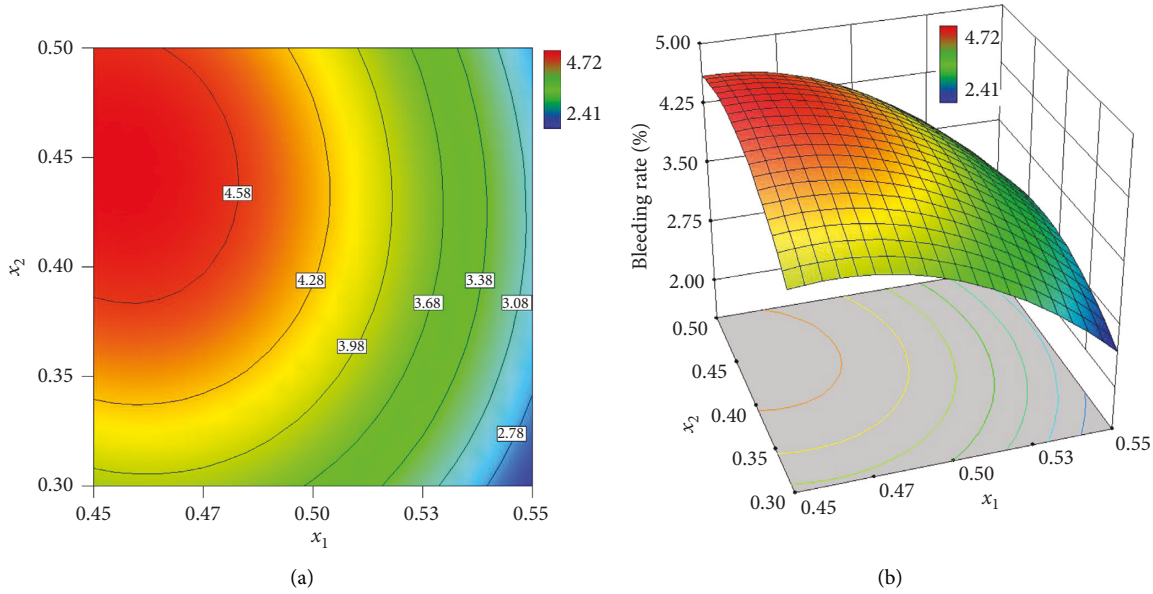

Figure 11: Interaction influence of x_1 and x_2 on bleeding ratio. (a) Two-dimensional diagram. (b) Three-dimensional diagram.

with the increase of the wet fly ash/aggregate ratio. For example, when Talbol gradation index and wet fly ash/aggregate ratio are 0.3 and 0.49, respectively, the maximum of 28 d strength is 3.58 MPa. Moreover, with the increase of gradation, the maximum of 28 d strength increases gradually, and the maximum of wet fly ash/aggregate ratio increases accordingly. For example, when Talbol gradation index and wet fly ash/aggregate ratio are 0.45 and 0.52, respectively, the maximum of 28 d compressive strength reaches 3.85 MPa, which is significantly higher than that with the Talbol gradation of 0.3. In addition, the contour diagram demonstrates that when the gradation and wet fly ash/aggregate ratios are 0.48 to 0.50 and 0.48 to 0.55, respectively, high compressive strength can be obtained.

In Figure 13, the interaction influences of wet fly ash/aggregate ratio and the percentage of water reducing agent on 28 d compressive strength are depicted, in which Talbol gradation index of construction waste is fixed at 0.4. When the dosage of water reducing agent is small, the strength increases gradually with the increase of wet fly ash/aggregate ratio. When the dosage of water reducing agent is 0.60 and the wet fly ash/aggregate ratio is 0.55, the 28 d strength is 3.70 MPa. If the percentage of water reducing agent in cement exceeds 0.63%, with the increase of wet fly ash/aggregate ratio, the strength increases at first and then decreases, and the increase or decrease rate gets smaller around the peak. When the dosage of water reducing agent and the wet fly ash/aggregate ratio are 0.8 and 0.55,

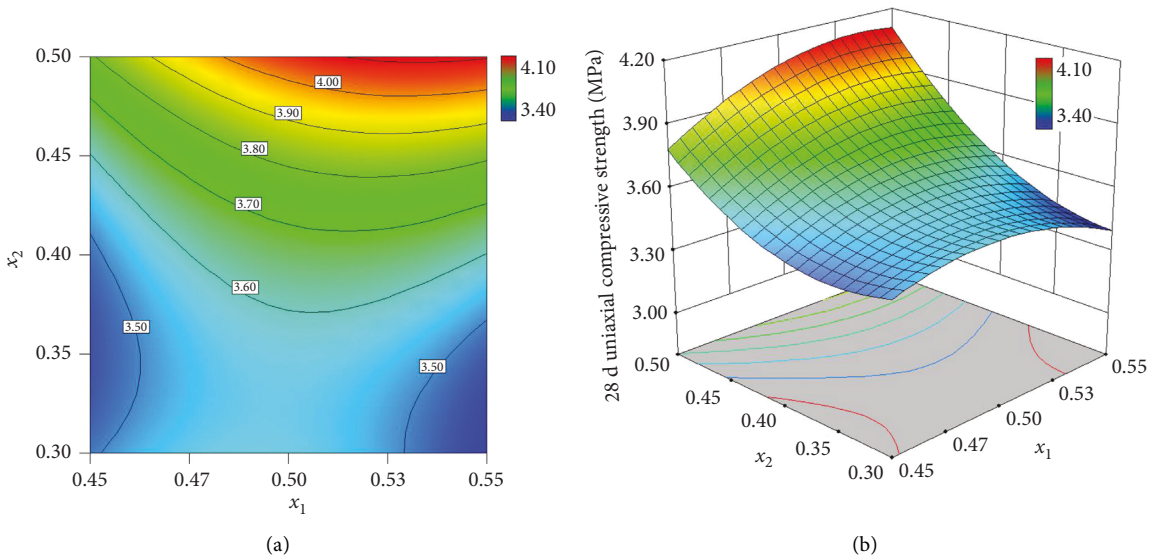

FIGURE 12: Interaction influence of x_1 and x_2 on 28 d compressive strength. (a) Two-dimensional diagram. (b) Three-dimensional diagram.

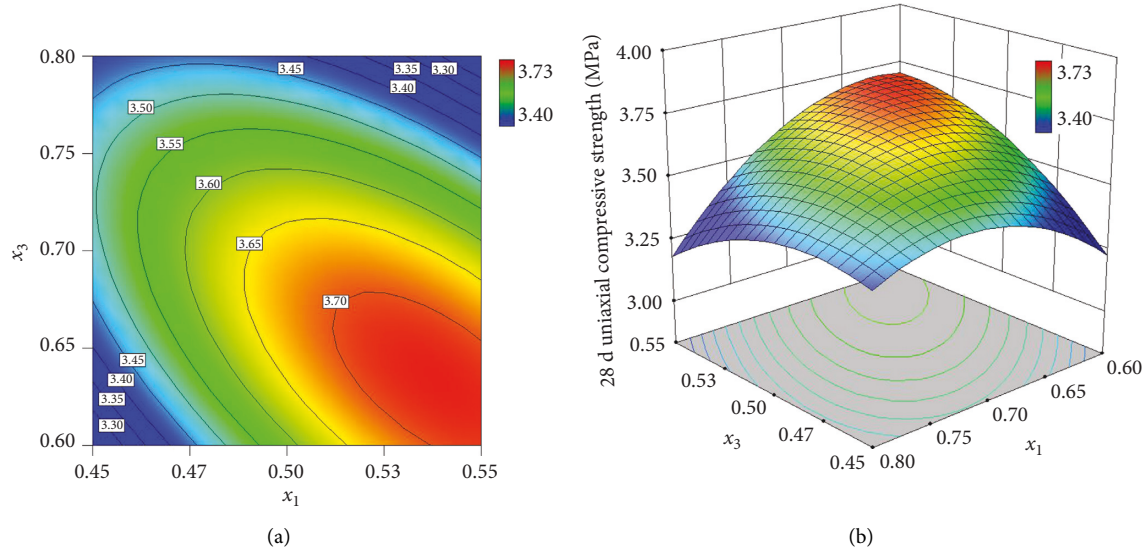

FIGURE 13: Interaction influence of x_1 and x_3 on 28 d compressive strength. (a) Two-dimensional diagram. (b) Three-dimensional diagram.

respectively, the 28 d strength is 3.17 MPa. At a low wet fly ash/aggregate ratio, the strength increases at first and then decreases slightly with the increase of water reducing agent. However, when the wet fly ash/aggregate ratio increases gradually, the increase gets smaller, followed by an increasingly obvious decrease. As shown in the contour diagram, when the wet fly ash/aggregate ratio and dosage of water reducing agent are in the ranges of 0.52 to 0.55 and 0.60 to 0.67, respectively, the maximum of compressive strength can be derived.

3.3. Multiobjective Optimization and Model Verification. The cost of filling material is an important factor affecting the economic benefit of mine. As long as the physical property of filling material is ensured, reducing the cost of filling material is an important way to improve the benefit of mining.

At present, Longhu Mine of Qitaihe Co., Ltd. of Longmei Group is using the filling mining method to mine the coal below buildings. The filling material used must satisfy certain performance specifications, specifically, with slump, bleeding ratio, and the 28 d compressive strength being 210–220 mm, less than 5%, and greater than 3 MPa, respectively. If taking the Longhu Mine as the case to demonstrate the economic optimization of filling material, the following planning equation can be established:

$$220 \geq Y_1 \geq, Y_2 = \min, Y_3 = \max. \quad (8)$$

Table 8: Price of partial filling material mix ratio.

No.	x_1	x_2	x_3 (%)	M_c	M_f	M_w	M_s	Slump (mm)	Bleeding ratio (%)	28 d compressive strength (MPa)	Price (yuan/m^3)
1#	0.507	0.500	0.678	0.817	0.414	0.460	0.147	210	3.99	4.10	103.7
2#	0.509	0.500	0.686	0.816	0.415	0.460	0.147	210	3.95	4.11	104.0
3#	0.513	0.498	0.697	0.814	0.418	0.460	0.147	210	3.92	4.09	104.5
4#	0.506	0.488	0.670	0.818	0.414	0.460	0.147	210	4.03	4.04	105.0
5#	0.511	0.478	0.680	0.815	0.416	0.460	0.147	210	4.00	3.99	106.5
6#	0.517	0.448	0.709	0.812	0.420	0.460	0.147	210	4.01	3.83	110.9
7#	0.505	0.401	0.675	0.818	0.413	0.460	0.147	210	4.14	3.68	115.8
8#	0.504	0.369	0.700	0.819	0.413	0.460	0.147	210	4.11	3.60	120.5
9#	0.501	0.352	0.714	0.821	0.411	0.460	0.147	210	4.11	3.56	123.1
10#	0.497	0.314	0.766	0.823	0.409	0.460	0.147	210	4.03	3.44	129.4

In the optimization module of Design-Expert 10.0.3 software, 77 groups of solutions satisfying the equation can be obtained by setting the value range of response value according to the above planning equation. The minimum cost of filling material per unit volume is taken as the optimization objective, namely, $f_{\min}$ (yuan/m^3), and the optimization model is established as shown in the following formula:

$$\begin{cases} \dfrac{M_c}{2.62} + \dfrac{M_f}{2.3} + \dfrac{M_w}{1} + \dfrac{M_s}{3.1} + \dfrac{M_s x_3}{2.1} = 1, \\ \dfrac{M_s}{M_c + M_f + M_s + M_w + M_s x_3} \times 100\% = 8\%, \\ \dfrac{M_w}{M_c + M_f + M_s + M_w + M_s x_3} \times 100\% = 25\%, \\ \dfrac{M_f}{M_c} = x_1, \\ x_4 = -150 x_2 + 95, \\ f_{\min} = x_4 M_c + 10 M_f + 3.2 M_w + 420 M_s + 20000 M_s x_3, \end{cases} \tag{9}$$

where x_1 is the ratio of wet fly ash versus construction waste; x_2 is Talbol gradation index of construction waste; x_3 is the mass percentage of water reducing agent versus cement; x_4 is the price of construction waste; M_c, M_f, M_w, and M_s, are the masses of construction waste, wet fly ash, water, and cement per cubic metre of filling material. The mass concentration of solid material in the filling material is 75%. The masses of water and cement account for 25% and 8%, respectively, of filling material.

Based on current raw material prices, cement, water reducing agent, wet fly ash, and industrial water are 420, 20000, 10, and 3.2 yuan/t, respectively. The prices of construction waste with n of 0.5 and 0.3 are 20 and 50 yuan/t, respectively, and the price of construction waste of other Talbol gradation indexes can be obtained by interpolation formula ($x_4 = -150x_2 + 95$). The 77 groups of solutions were substituted into the optimization model (formula (8)), and the results were calculated using Matlab (see Table 8 for some of the results). From the results, it can be seen that the lowest price ($f_{\min}$) per cubic metre of filling material is 103.7 yuan for $x_1 = 0.507$, $x_2 = 0.5$, and $x_3 = 0.678\%$. The model predicts that the slump, bleeding ratio, and 28 d compressive strength are 210 mm, 3.99%, and 4.10 MPa, respectively. Indeed, the filling materials with these mix ratios were tested experimentally, and the slump, bleeding ratio, and 1 d, 7 d, and 28 d compressive strength are 215 mm, 4.00%, and 4.08 MPa, respectively, indicating that the results addicted by the model highly match the actual results and can meet requirements of field construction.

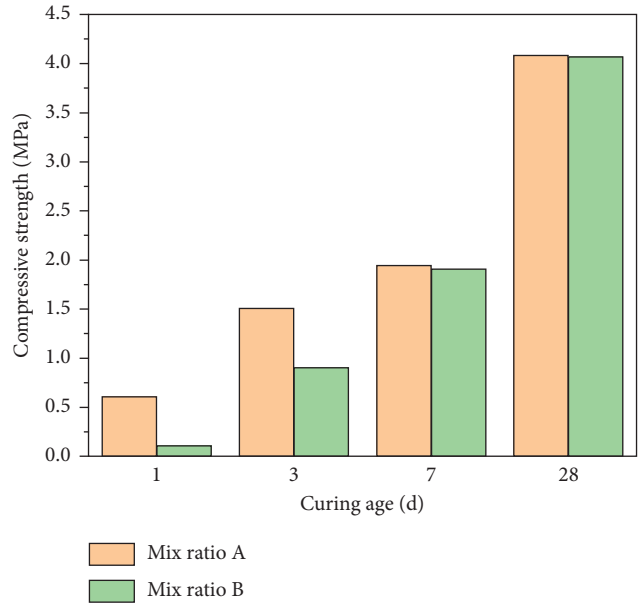

Figure 14: Compressive strength of various curing ages of the optimal mix ratio of filling material.

3.4. Analysis of Filling Material at Different Curing Ages. In Figure 14, mix ratio A shows the compressive strength at the curing ages for the optimum mix ratio of filling material. Mix ratio B is the compressive strength at each curing age after replacing 42.5# sulphate aluminate cement with 42.5# Portland cement in the optimum mix ratio of filling material. Figure 14 shows that the one-day compressive strength of mix ratio A is 6 times that of mix ratio B, and the three-day

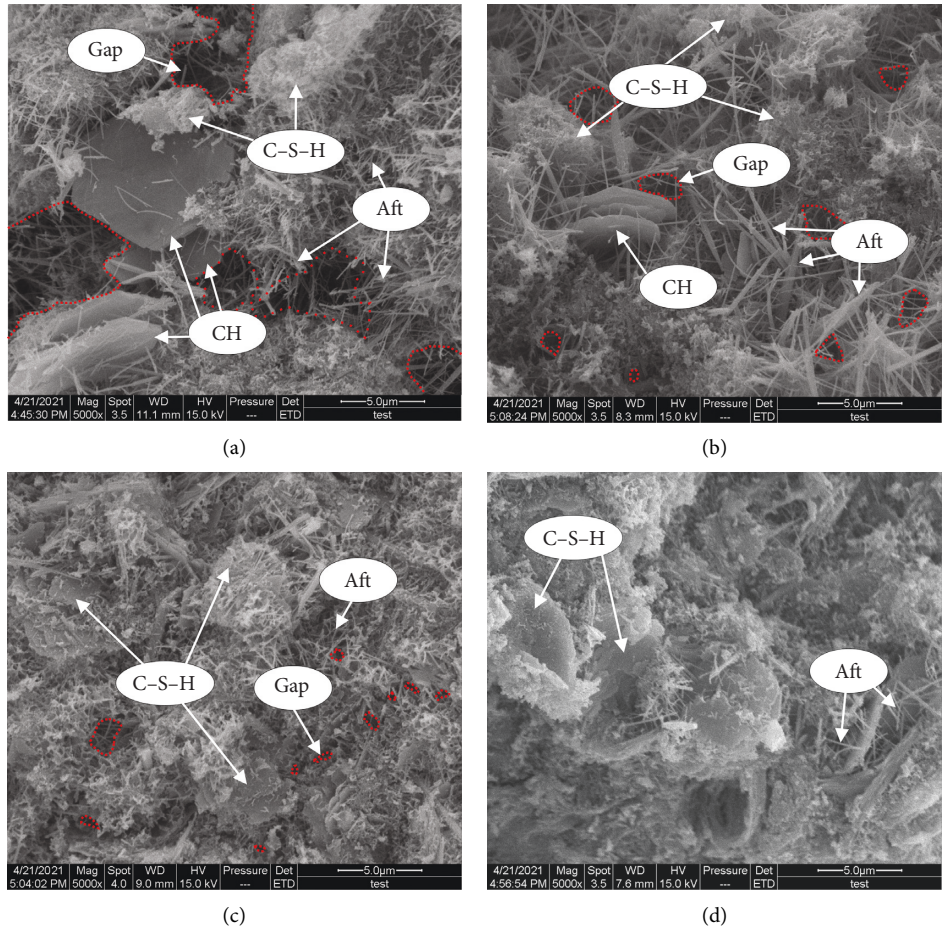

Figure 15: SEM photos of the hydration products of the optimum mix ratio of filling material at different curing ages. (a) 1 d curing age. (b) 3 d curing age. (c) 7 d curing age. (d) 28 d curing age.

compressive strength of mix ratio A is 1.67 times that of mix ratio B; after that, the compressive strengths of the two mix ratios are basically the same.

The SEM photos of the hydration products of the optimum mix ratio of filling material at curing ages of 1 d, 3 d, 7 d, and 28 d are shown in Figure 15. The sulphate aluminate cement mainly produces calcium vanadate (Aft), and the Portland cement hydrates mainly produce hydrated calcium silicate (C-S-H) gelation, both of which precipitate calcium hydroxide (CH). When the curing age of the filling material is 1 d (Figure 15(a)), the gaps between the hydration products are significant, a large number of needle-like Aft appear, and there is a small amount of C-S-H gelation, while a large number of CH can be seen, and the morphology of CH is a regular plate hexahedron, the surface of which has a crystal luster and good crystallinity. When the age of the filling material is 3 d (Figure 15(b)), the gaps between the hydration products become smaller; the size of the Aft increases significantly and becomes "rod" shaped; the hydration of Portland cement produces a certain amount of C-S-H gelation; CH becomes less, because CH reacts chemically with the active SiO_2, Al_2O_3, and so forth in fly ash. As shown from Figures 15(a) and 15(b), the increase in compressive strength of the filling material within 3 d of the curing age is mainly due to the hydration of the sulphate aluminate cement to produce a large amount of Aft. At the curing age of 7 d for the filling material (Figure 15(c)), the gaps between the mid-hydration products are smaller, a significant number of filamentous C-S-H encapsulates the Aft, and the shape of CH hexahedron is not obvious, and the crystallinity of CH is worse than that in Figure 15(b). At the curing age of 28 d (Figure 15(d)), the filling material is dense and the needle stick Aft is largely encapsulated by the gel. Only a small amount of Aft can be seen, and CH crystals are basically invisible. From Figures 15(a) and 15(b), it can be seen that the compressive strength of the filling material at the curing age of 7 d to 28 d is mainly due to the large amount of C-S-H gelation which is produced by the hydration of Portland cement.

4. Conclusions

The response surface methodology (RSM) is using slump, bleeding ratio, and 28 d uniaxial compressive strength of the filling material as response variables, as well as using wet fly ash/aggregate ratio, Talbol gradation index of recycled aggregate, and dosage of water reducing agent as factors, which has optimized the mix ratio of construction waste cemented filling material. The main conclusions are as follows:

(1) The reliable and accurate response surface model of slump, bleeding ratio, and 28 d compressive strength was established, with the determination coefficient greater than 0.93 and the coefficient of variation (CV) less than 5%. The relative errors between the response surface model and the experimental results were within 4%, indicating a good fitting.

(2) The wet fly ash/construction waste ratio, Talbol gradation index of recycled aggregate, and dosage of water reducing agent had the most significant effects on bleeding ratio, 28 d compressive strength, and slump, respectively. The interaction of wet fly ash/construction waste ratio and Talbol gradation index of recycled aggregate had an obvious effect on the three response values, and the interaction of wet fly ash/construction waste ratio and water reducing agent proportion significantly influenced the 28 d compressive strength.

(3) The optimal mix ratio of filling material was obtained: the wet fly ash/construction waste ratio was 0.507, Talbol gradation index of recycled aggregate was 0.5, and dosage of water reducing agent was 0.678%. Experimentally, the filling material with the optimal mix ratio yielded slump of 215 mm, bleeding ratio of 4.00%, and 28 d compressive strength of 4.08 MPa, which meet the actual needs of mining.

(4) The hydration of sulphate aluminate cement produces a large amount of Aft, which can obviously improve the compressive strength of the filling material in 3 d. The hydration of Portland cement produces a large amount of C-S-H gelation, which is the main source of the compressive strength of the filling material from 7 d to 28 d.

Data Availability

The data used to support the findings of this study are available from the corresponding author upon request or change this to the fixed mode of journals.

Conflicts of Interest

The authors declare that they have no conflicts of interest.

Acknowledgments

The work was supported by Scientific and Technological Key Project of "Revealing the List and Taking Command" in Heilongjiang Province (Grant no. 2021ZXJ02A03) and Heilongjiang Provincial Natural Science Foundation of China (Grants nos. LH2020E121andLH2019E119).

References

[1] S. G. Wang, Q. Sun, J. W. Qiao, and H. H. Schobert, "Discussion on the geological guarantee of green coal mining," *Journal of China Coal Society*, vol. 45, no. 1, pp. 8–15, 2020.

[2] H. P. Kang, G. Xu, B. M. Wang, and S. Li, "Forty years development and prospects of underground coal mining and strata control technologies in China," *Journal of Mining and Strata Control Engineering*, vol. 1, no. 1, pp. 232–237, 2019.

[3] G. F. Wang, "Innovation and development of safe, high-efficiency and green coal mining technology and equipments," *Coal Mining Technology*, vol. 18, no. 5, pp. 1–5, 2013.

[4] J. G. Liu, X. W. Li, and T. He, "Application status and development of filling mining in coal mine in China," *Journal of China Coal Society*, vol. 45, no. 1, pp. 141–150, 2020.

[5] J. L. Xu, "Research and progress of green mining in coal mine in 20 years," *Coal Science and Technology*, vol. 48, no. 9, pp. 1–15, 2020.

[6] B. N. Hu, "Backfill mining technology and development tendency in China coal mine," *Coal Science and Technology*, vol. 40, no. 11, pp. 1–5, 2012.

[7] K. J. Jia and G. M. Feng, "Backfill mining technology with ultra high water material in coal mine and outlook," *Coal Science and Technology*, vol. 40, no. 11, pp. 6–9, 2012.

[8] B. G. Yang and J. Yang, "Development and selection on filling technology of coal mine," *Mining Research and Development*, vol. 35, no. 5, pp. 11–15, 2015.

[9] K. Cheng, B. G. Yang, B. G. Zhang, D. Li, J. Yang, and R. Zhang, "Present situation and development direction of filling mining technology in coal mines in China," *Coal Technology*, vol. 37, no. 3, pp. 73–76, 2018.

[10] X. K. Sun, "Present situation and prospect of green backfill mining in mines," *Coal Science and Technology*, vol. 46, no. 9, pp. 48–54, 2020.

[11] Z. H. Li, "Discussion on the present situation and development suggestions of the utilization of construction waste resources in China," *China Resources Comprehensive Utilization*, vol. 36, no. 10, pp. 74–77, 2018.

[12] J. Zhou, "Present situation and treatment process of construction and demolition waste at home and abroad," *Guangdong chemical*, vol. 48, no. 20, pp. 193-194, 2021.

[13] H. L. Lu, "Analysis of the problem and outlet of China's construction waste," *Environment and Sustainable Development*, vol. 43, no. 3, pp. 45–48, 2018.

[14] Y. B. Xu, Y. Li, and B. Fan, "The current situation, problems and suggestions of construction waste recycling industry in China," *Wall Materials Innovation and Energy Saving in Building*, vol. 12, no. 1, pp. 56–59, 2019.

[15] Y. Liu, H. Guo, W. Chen, and Y. Huang, "Experimental study on proportion optimization of construction waste paste filling materials," *Safety In Coal Mines*, vol. 48, no. 6, pp. 65–68, 2017.

[16] H. Q. Zhang, Y. Liu, and Q. F. Wang, "Study on performance of paste filling with urban construction waste," *Mining Research and Development*, vol. 34, no. 4, pp. 37–39, 2014.

[17] M. Y. Jiang, T. C. Li, Z. Li, H. Y. Wang, and Y. Z. Sun, "Orthogonal test study on the preparation of filling paste with construction waste aggregate," *Bulletin of the Chinese Ceramic Society*, vol. 34, no. 10, pp. 2948–2953, 2015.

[18] W. C. Qiu, F. G. Wang, S. J. Liu, and W. Jie, "Effect of particle size on the strength of construction waste slurry backfill material," *Journal of Shandong University of Technology*, vol. 30, no. 6, pp. 40–43, 2016.

[19] H. Li, Y. Liu, K. Wang, and R. Raghavan, "Experimental study on physical properties of construction waste aggregate-coarse fly ash-based cement filling," *Safety In Coal Mines*, vol. 50, no. 12, pp. 60–63, 2019.

[20] H. F. Liu, J. X. Zhang, N. Zhou et al., "Investigation of spatial stratified heterogeneity of cemented paste backfill characteristics in construction demolition waste recycled

aggregates," *Journal of Cleaner Production*, vol. 249, Article ID 119332, 2020.

[21] B. G. Yang, J. Y. Jin, X. D. Yin, and H. Yang, "Effect of concentration and suspension agent (HPMC) on Properties of coal gangue and fly ash cemented filling material," *Shock and Vibration*, vol. 2021, Article ID 6643773, , 2021.

[22] Y. S. Tang, L. F. Zhang, and H. Y. Lu, "Study on proportion optimization of coal-based solid wastes filling materials," *Journal of Mining Science and Technology*, vol. 4, no. 4, pp. 328–336, 2019.

[23] A. P. Cheng, F. S. Dong, P. F. Shu, and X. Fu, "Mechanical properties and acoustic emission characteristics of continuous graded cemented backfill," *Journal of Huazhong University of Science and Technology (Nature Science Edition)*, vol. 49, no. 8, pp. 47-48, 2021.

[24] W. X. Chen, F. Y. Li, and Q. Y. Shan, "Rheological properties behind fly-ash-based cement filling material," *Journal of Heilongjiang University of Science & Technology*, vol. 29, no. 1, pp. 105–109, 2019.

[25] S. L. Shu, G. C. Li, G. L. Liu et al., "Ratio Optimization of Slag-Based Solid Waste Cementitious Material Based on response surface method," *Bulletin of the Chinese Ceramic Society*, vol. 40, no. 1, pp. 187–192, 2021.

[26] S. H. Yin, S. Hao, L. Zhou, Y. Z. Kou, X. W. Li, and A. Belibi, "Research on strength regression and slurry optimization of cemented backfill based on response surface method," *Journal of Central South University (Science and Technology)*, vol. 51, no. 6, pp. 1596–1600, 2020.

[27] S. H. Liu, K. H. Fang, H. L. Shen, and X. Y. Wang, "Influence of fly ash on water requirement, landslide degree and workability of concrete," *Fly Ash Comprehensive Utilization*, vol. 2, no. 3, pp. 47-48, 2005.

[28] T. Li, X. L. Wang, M. Li, D. Y. Nan, Q. Y. Shan, and W. X. Chen, "Synergy between suspending agent and air entraning agent in cement slurry," *Revista Romana de Materiale*, vol. 41, pp. 344–353, 2020.

[29] Z. G. Fu, D. P. Qiao, Z. L. Guo, X. Jincheng, H. Fei, and W. Jiaxin, "Experimental research on mixture proportion and strength of cemented hydraulic fill with waste rock and eolian sand based on RSM-BBD," *Journal of China Coal Society*, vol. 43, no. 43, pp. 695–700, 2018.